CHEMICAL ENGINEERING TRANSACTIONS

VOL. 120, 2025

A publication of AIDIC

The Italian Association of Chemical Engineering
Online at www.cetjournal.it

Guest Editors: Bing Shen How, Viknesh Andiappan, Denny K.S. Ng, Hon Loong Lam, Petar S. Varbanov
Copyright © 2025, AIDIC Servizi S.r.l.
ISBN 979-12-81206-21-2; **ISSN** 2283-9216

DOI: 10.3303/CET25120009

Economic Evaluation of a Stage Compression Heat Pump System for Industrial Applications

Guillermo Martínez-Rodríguez[a,*], Amanda L. Fuentes-Silva[a], Juan-Carlos Baltazar[b]

[a]Department of Chemical Engineering, University of Guanajuato, Guanajuato 36050, Mexico
[b]Texas A&M Engineering Experiment Station (TEES), Texas A&M University, College Station 3581, U.S.A.
guimarod@ugto.mx

A compressor represents 80 % of the cost of a heat pump, and the heat pump represents 70 % of the cost of a coupled system heat pump-solar thermal installation. A single heat pump was designed, another with two-stage compression and a third with three-stage; the heat source is solar thermal energy at 70 °C. A dairy process was selected that consumes 880.45 kW at 95 °C and the working fluids R600a and R1336mzz(E) were used. The solar thermal installation was designed with average environmental conditions of the winter period in Guanajuato city, Mexico. R600a achieved the best results in all configurations. The COP of the heat pump showed an increase of up to 16 % and when operating with two-stage compression, and 18 % with three-stage. The cost of the heat pump with one or two-stage compression was reduced by 35 % when the solar source temperature rose from 40 to 70 °C. The proposed approach contributes to decarbonization with lower energy costs compared to the costs of using fossil fuels.

1. Introduction

Heat pumps are devices that use low-quality heat and deliver high-quality heat; industrial heat pumps produce >200 kWth. They have been identified as a crucial technology for industrial decarbonization, equivalent to 15.1 $GtCO_{2e}$ by 2023. The heat pumps are also highly efficient and have a low carbon footprint (UNEP, 2024). According to the International Renewable Energy Agency (IRENA), fewer than 1×10^6 heat pumps were installed in the industry in 2020. It is expected that by 2050, the total number of industrial heat pumps installed worldwide will reach 80×10^6 (IRENA, 2023), meaning that heat pumps will supply 30 % of the heat demand in light industries (EHPA, 2023a). In Europe, heat accounts for 60 % of industrial energy consumption (EHPA, 2023b), and of this, approximately 37 % is below 200°C (IEA, 2022). The heat pump market was valued at USD 9.5 billion in 2023 and is projected to grow at a compound annual growth rate of 5.8 % until 2030 (TechNavio, 2025). These systems allow the integration of low-temperature heat sources, such as solar thermal energy, to produce solar process heat. Coupled heat pump-solar thermal installation systems (hereafter referred to as "coupled systems") have expanded their applications. Solar thermal-assisted heat pumps raise the source temperature to 144 °C at the sink, increasing the efficiency of an organic Rankine cycle by up to 14.5 % according to Martínez-Rodríguez et al. (2024). For large-scale industrial heat pumps, total investment costs of USD 381,404 (Heating capacity: 200 kW, T_{sink}: 80 °C, R134A, Heat pump model: HTHP1); USD 451,831 (Heating capacity: 1000 kW, T_{sink}: 150 °C, R717, Heat pump model: HTHP4); and USD 1,915,438 (Heating capacity: 3250 kW, T_{sink}: 150 °C, R717, Heat pump model: SHP25) are reported (Bhadbhade et al., 2024). In reported coupled systems, the investment cost ranges between USD 0.29/MW and USD 2.79/MW (Jørgensen et al., 2019). The levelized energy cost was estimated at 0.0409 USD/kWh for a 2G anhydrous bioethanol production process requiring 636.79 kW of thermal energy at a temperature of 105 °C (process hot water) and 0.0799 USD/kWh for a dairy process requiring a heat load of 880 kW at a temperature of 85 °C (service water) (Martínez Rodríguez et al., 2023). The investment cost of the compressor represents 92 % of the total cost of the heat pump (Díaz-de-León et al., 2024). In solar thermal-assisted systems, the cost of the heat pump accounts for 35 - 60 % of the total system cost, depending on the ΔT_{lift} (Díaz-de-León et al., 2024). Depending on the heat pump model and compressor type, for the same heat load and sink temperature, the cost can vary between 23 – 40 % (Schlosser et al., 2020).

Paper Received: 18/04/2025; Revised: 5 September 2025; Accepted: 10 October 2025
Please cite this article as: Martínez-Rodríguez G., Fuentes-Silva A.L., Baltazar J.-C., 2025, Economic Evaluation of a Stage Compression Heat Pump System for Industrial Applications, Chemical Engineering Transactions, 120, 49-54 DOI:10.3303/CET25120009

Two-stage vapor-compression heat pumps operate with a larger temperature difference between the evaporator and condenser (ΔT_{lift}), resulting in higher efficiency. Qiu et al. (2024) modeled and optimized a two-stage vapor-compression heat pump system with a configuration including a closed economizer cycle and interstage refrigerant injection. In the two-stage heat pump, the intermediate temperature and the displacement ratio between the low-pressure compressor and the high-pressure compressor are important parameters influencing the COP. The maximum coefficient of performance (COP) was 2.85 and 2.7 at an ambient temperature of −30 °C with R290 and R410A, respectively. Arpagaus et al. (2016) proposed a novel two-stage heat pump system with two heat sources at two different temperature levels (5 °C and 30 °C) to provide hot water at 55 °C (6.5 kW). The results show that coefficient of performance (COP = 4.3) improvements of between 20 % and 30 % can be achieved, depending on the temperature levels of the heat sources. The coefficient of performance increases with higher source temperatures and lower condenser temperatures (pressure ratio of 2.3 for the first stage compressor and 2.38 for the second stage compressor).
Multistage compressor heat pumps are systems with two or more compression stages in the same cycle. Multistage compression is recognized as providing high COPs (IEA, 2014). Currently, multistage compression systems, connected in series or parallel, using single- or multi-stage compressors with injection ports between the compression chambers are a mature technology. Multistage compressor cycles are a common configuration in refrigeration (15 to 0 °C), freezing (-20 to -40 °C), and deep freezing (below -40 °C) (He et al., 2023).
This work analysed a coupled heat pump-solar thermal system with two and three compression stages in series, with an intermediate expansion tank between the heat pump expansion valves. R600a and R1336mzz(E), both refrigerants with low environmental impact, were also selected as working fluids. The objective was to improve the coefficient of performance (COP) by reducing the compression load of the proposed system for an industrial dairy process, with a competitive energy cost.

2. Methodology

A dairy process is being studied that operates in batches for 12 hours per day (6:00 h – 18 h). 20,000 L of milk need to be pasteurized (8:00 h –13:00 h), and a heat flow of 880 kW must be provided. To achieve this, 45 m^3 of hot water must be produced at a temperature of 95 °C. The total heat load supplied by the boiler is 4,400 kWh (15,840 GJ).

2.1 Design of a two- and three-stage compression system for a heat pump

The performance of a single-stage heat pump deteriorates when operating with low evaporation temperatures and high condensation temperatures. Under these conditions, the compressor operates at high pressure ratios, decreasing its efficiency; consequently, the COP and heat capacity of the heat pump are reduced, and the compressor discharge temperature increases, causing operational problems. To overcome the limitations of the single-stage compression cycle, a two-stage compression cycle with steam injection is proposed. In this work, steam injection between two compression stages is performed using a flash tank, as shown in Figure 1(a). This device is used to vaporize the refrigerant injected during the compression process. Figure 1(b) shows the pressure-enthalpy diagram of the two-stage heat pump. In this system, the refrigerant expands to an intermediate pressure at the condenser outlet. The heat supplied by the heat pump to the process, $\dot{Q}_{cond}$, is defined by the heat duty required by the process (880 kW). The heat pump outlet temperature also depends on the process target temperature (95 °C). Based on these two system operating criteria, the refrigerant type and the operating temperature of the heat pump evaporator are selected. Eq(1) provides the heat duty on the condenser.

$$\dot{Q}_{cond} = \dot{m}_{R2}(h_5 - h_4) \tag{1}$$

Where, $\dot{m}_{R2}$, is the mass flow rate of the working fluid in the high-pressure stage, kg/s; h_4 and h_5, are the enthalpies of the superheated and subcooled refrigerant, at the inlet and outlet of the condenser, kJ/kg.
The heat absorbed by the evaporator, $\dot{Q}_{eva}$, is supplied by the solar thermal installation. It is designed to operate under average winter conditions for the city of Guanajuato. Eq(2) is used to calculate the heat duty required for this equipment.

$$\dot{Q}_{evap} = \dot{m}_{R1}(h_1 - h_8) \tag{2}$$

Where, $\dot{m}_{R2}$, is the mass flow rate of the working fluid in the low-pressure stage, kg/s; h_8 and h_1, are the enthalpies of the refrigerant, at the entrance and exit of the evaporator, kJ/kg
Power consumption by the heat pump, $\dot{W}_{net}$, is the sum of $\dot{W}_{el,low}$ and $\dot{W}_{el,high}$, electrical input compressor in the low- and high- pressure stage, kW, is expressed in Eq(3-4).

$$\dot{W}_{el,low} = \dot{m}_{R1}(h_2 - h_1) \quad (3)$$

$$\dot{W}_{el,high} = \dot{m}_{R2}(h_4 - h_9) \quad (4)$$

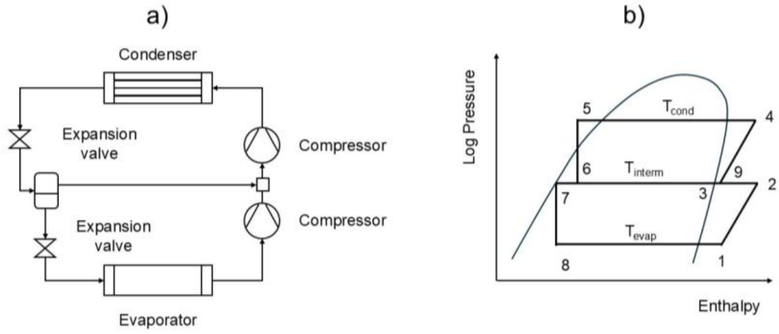

Figure 1: Operation diagram of a heat pump with two compression stages: a) operation diagram and b) corresponding p-h diagram.

Where, $h_2 - h_1$, is the enthalpy difference at the compressor outlet and inlet in the low-pressure stage, kW; $h_4 - h_9$, it is the enthalpy difference at the outlet and inlet of the high-pressure compressor. Coefficient of performance (COP) of a heat pump is defined with Eq(5), which describes the relationship between the heating energy generated and the electricity required.

$$COP = \frac{\dot{Q}_{cond}}{\dot{W}_{el,low} + \dot{W}_{el,high}} \quad (5)$$

The following heat pump operating conditions are considered. In the compression stages, an isentropic efficiency of 0.85 is assumed. The expansion process is isenthalpic, and pressure drops across the heat exchangers are neglected. The overall heat transfer coefficient values used are 1.2 and 1.1 kW/m^2 K, for the evaporator and condenser, respectively. Furthermore, the superheating (10 °C) and subcooling (10 °C) degrees are constant. The heat pump heat source temperature is 70 °C. The evaporation temperature is 10 °C lower than the heat source temperature. R600a and R1336mzz(E) are selected as working fluids. Table 1 presents a comparison of the characteristics and properties of the refrigerants selected in the study. R600a is a conventional refrigerant while R1336mzz(E) is a low-environmental impact hydro-fluor-olefin (HFO).

Table 1: Properties of selected refrigerants.

Refrigerant	$T_{critical}$ (°C)	$P_{critical}$ (MPa)	Safety group	ODP	GWP	Family	Atmospheric Lifetime
R600a	134.70	3.64	A3	0	4	HC	< 1 y
R1336mzz(E)	137.70	3.15	A1	0	18	HFO	67 d

The same considerations apply to the design of a heat pump with three compression stages.
The proposed thermodynamic model has been validated with data reported in literature.

2.2 Design of the low-temperature solar thermal installation

The design of the solar thermal installation consists primarily of a network of solar collectors and a thermal storage tank. The sizing of this system considers the average winter weather conditions found in Guanajuato City, Mexico (21.01 N, 101.26 W, altitude 2045 m), as shown in Table 2.

Table 2: Average weather conditions for the winter period.

Irradiance (W/m^2)	Irradiation (kWh/m^2/d)	Ambient temperature (°C)	Wind velocity (m/s)	Light hours (h)
473.33	5.89	20.90	1.69	12.45

To design the low-temperature solar collector network, data from a commercially available flat-plate collector are taken, and for the thermal storage system, a thermally insulated tank marketed for these applications is considered. The sizing of the solar thermal installation is based on the methodology proposed by Martínez-Rodríguez et al. (2019), where the size and arrangement of the network must meet the heat duty and temperature level required by the process.

2.3 Estimating the energy cost of a coupled heat pump – solar thermal installation system

The cost assessment considers only the capital cost of the main equipment of the coupled heat pump-solar thermal system. The total cost of the coupled system, $C_{T\,HP-SOLAR}$, is given by Eq(6).

$$C_{T\,HP-SOLAR} = C_{EVAP} + C_{COMP} + C_{COND} + C_{SC} + C_{ST} \tag{6}$$

The main components of the solar thermal installation are the cost of the flat-plate solar collector network, C_{SC}; and the cost of the hot water storage system, C_{ST}, USD. For the heat pump, its main components are heat exchangers, C_{COND} and C_{EVAP}; and the compressors, C_{COMP}, USD, according to the compression stages. Table 3 presents the ratios of the costs of the main equipment based on the most representative variable for each piece of equipment.

Table 3: Cost ratios of major equipment.

Cost function	Variable, units
$C_{SC} = 200 \cdot A_{capt}$	A_{capt}, solar absorber area, m^2.
$C_{ST} = 13280 \left(\frac{V_{ST}}{15.4}\right)$	V_{st}, storage volume, m^3.
$C_{COMP} = 4896.57 \cdot \dot{W}_{comp}$	$\dot{W}_{comp}$, Power consumption, kW.
$C_{COND} = C_{EVAP} = 516.621 A_{hx} + 268.45$	A_{hx}, heat exchange area, m^2.

The levelized cost of energy (LCOE) is used as an indicator to evaluate the profitability of the proposed system, USD/kWh, given by Eq(7). This indicator relates the costs of investment, $C_{T\,HP-SOLAR}$, USD; operation and maintenance, $C_{O\&M}$, USD (20 % installation, 45 % operation and maintenance, 20 % contingencies from investment cost); and electricity use, C_{EL}, USD, with respect to the net energy production of the system throughout its useful life, E_{NET}, kWh.

$$LCOE = \frac{CFR \cdot C_{T\,HP-SOLAR} + C_{O\&M} + C_{EL}}{E_{NET}} \tag{7}$$

CFR is the capital recovery factor (plant life of 25 years and interest rate of 8 %).
Net Present Value (NPV) represents the value that can be realized from the investment and is used to assess the economic viability of an investment is defined in Eq(8).

$$NPV = \sum_{i=1}^{i=n} \frac{S_i}{(1+r)^i} - C_{T\,HP-SOLAR} \tag{8}$$

where i is the lifespan of the plant; S_i is the annual savings, USD; r = 20 % is the discount (interest); and $C_{T\,HP-SOLAR}$, is the inicial outlay (investment), USD. IRR or r is the discount rate at which the present value of an investment's cash inflows equals the present value of its cash outflows. It represents the rate of return that makes the NPV of an investment zero.

3. Results and Discussion

The heat pump-solar thermal installation design parameter is set to produce 45 m^3 of hot water at 95 °C (4,400 kWh/d) for the milk pasteurization process throughout the year. The heat pump operating conditions were set with a condensation temperature of 105 °C and an evaporation temperature of 50 °C. The solar thermal installation was designed to deliver the heat load at 70 °C. The design variables analysed in this work are the compression stages in the heat pump and the working fluid used. Table 4 shows the results of the studied designs and the main parameters of the proposed system: the pressure ratio in the compression stages, heat load on the evaporator, evaporation temperature, COP, absorber area of the solar thermal installation, volume of the hot water storage tank, and system costs. The COP of the heat pump using R600a working fluid for two- and three-stage compression is 5.2 and 5.3, which corresponds to an increase of 18 and 19 % compared to the COP of a single-stage compression heat pump. The cost of the heat pump is directly related to the compression of the refrigerant, due to the addition of an additional unit for the two-stage compression heat pump and two additional units for the three-stage compression system.
Heat pump COP results obtained using R1336mzz(E) for one-, two-, and three-stages compression in the heat pump are 3.8, 4.3, and 4.6. Increasing the number of compression stages increases the COP by 13 % and 21

% for two- and three-stages, respectively. The cost of adding one or two-stages compression impacts the investment cost and the LCOE. The results indicate that R600a has a higher COP compared to R1336mzz(E). For one-stage compression design, the increase is 18 %, for two-stage compression design, 21 %, and for three-stage compression design, 15 %. R600a has higher COP and the lowest energy cost.
The effect of source temperature is evaluated in the range of 40 - 70 °C using R600a and two compression stages in the heat pump. Figure 2a shows the COP trend for different evaporator temperatures. It is observed that using two compression stages, the COP is 21 % higher on average compared to one compression stage. Figure 2b shows the cost of the heat pump as the evaporator temperature varies using one- or two-stages compression. Increasing the source temperature from 40°C to 70°C reduces the cost of the heat pump by 35 % for one or two compression stages.

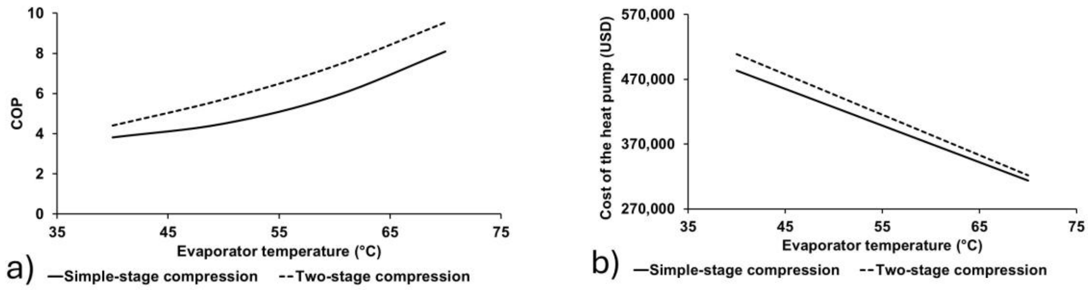

Figure 2: a) COP and b) Cost vs evaporator temperature with single- and two-stage compression heat pump, using R600a as working fluid.

The results of the financial indicators show that the solar thermal installation-heat pump system, with a single compression stage, using R600a presents the greatest economic viability: NPV = 213,977 USD, IRR = 25.8 %, Payback = 5.8 y. However, and in accordance with the evaluation criteria, all analyzed systems are profitable because the NPV is greater than zero and the IRR is greater than the cost of capital. The LCOE is estimated in a range of 0.0579–0.0630 USD per kWh with an average payback of 6.2 y.

Table 4: Design result of the coupled system for R600a and multiple compression stages.

Heat pump design/parameter	Single-stage compression heat pump		Two-stage compression heat pump		Three-stage compression heat pump	
Working fluid	R600a	R1336mzz(E)	R600a	R1336mzz(E)	R600a	R1336mzz(E)
Pressure ratio	3.2	4.0	1.94/1.63	2.22/1.80	1.35/1.46/1.60	1.67/1.60/1.50
Evaporator heat load, kW	685	649	706	671	708	701
Coefficient of Performance (COP)	4.5	3.8	5.2	4.3	5.3	4.6
Solar thermal installation absorber area, m^2	1527	1447	1574	1496	1579	1536
Thermal storage volume, m^3	47.0	44.6	48.5	46.1	48.6	47.3
C_{HP}, USD	420,381	475,297	430,239	496,445	494,285	525,173
$C_{SOLAR-INS}$, USD	348,530	330,213	359,215	341,407	360,233	350,565
Payback, y	5.8	6.1	6.0	6.3	6.5	6.6
NPV, USD	213,977	177,378	193,434	145,036	128,370	107,149
IRR, %	25.8	24.6	25.1	23.6	23.1	22.5
LCOE, USD/kWh	0.0579	0.0632	0.0567	0.0624	0.0598	0.0630

4. Conclusions

The heat pump's COP increases significantly by adding more than one-stage compression, reducing the power consumption. For two-stages compression it has highest COP of 5.2 and lowest heat pump investment capital cost of USD 430,239, using R600a. Increasing the source temperature reduces the cost of the heat pump by up to 35 %. The lowest energy cost is 0.0567 USD/kWh for R600a in all cases evaluated, the LCOE is competitive with that reported for fossil fuels, at 0.086 USD/kWh (TAMU, 2025).

References

Arpagaus C., Bertsch S., Javed A., Schiffmann J., 2016, Two-Stage Heat Pump using Oil-Free Turbocompressors - System Design and Simulation. International Refrigeration and Air Conditioning Conference. Paper 1602.

Bhadbhade N., Ong B. H.Y., Olsen D. G., Wellig B., Patel M. K., 2024, Assessment of CO_2 abatement potential of heat pumps using pinch analysis for the Swiss chocolate industry. Journal of Cleaner Production, 455, 142323.

Decarbonizing Food Processes with Industrial Heat Pumps. CIMCO Refrigeration, <cimcorefrigeration.com/resources/news/decarbonizing-food-processes-with-industrial-heat-pumps>, accessed 30.03.2025.

Díaz-de-León C.R., Fuentes-Silva A.L., Baltazar J.-C., Martínez-Rodríguez G., 2024, Performance Analysis of a Heat Pump Using Different Refrigerants to Supply Heat to Industrial Processes. Chemical Engineering Transactions, 114, 61-66.

EHPA Industrial heat pumps: decarbonising industry for a greener future, 2023a, Brussels, <ehpa.org/news-and-resources/news/industrial-heat-pumps-decarbonising-industry-for-a-greener-future/#:~:text=Heat%20pumps%20have%20been%20identified,technology%20can%20overcome%20these%20barriers.%E2%80%9D>, accessed 28.03.2025.

EHPA Subsidies for industrial heat pumps in Europe, 2023b, Brussels, <ehpa.org/wp EHPA_Subsidies-for-industrial-heat-pumps-in-Europe-1.pdf>, accessed 28.03.2025.

International Energy Agency, 2014, Application of Industrial Heat Pumps, Final Report, Part 1, Report no. HPP-AN35-1, IEA Heat Pump Programme.

International Energy Agency, 2022, Heat Pump Technologies (HPT). Annex58 Task 1: Technologies—State of the Art and Ongoing Developments for Systems and Components. <heatpumpingtechnologies.org/annex58/task1/>, accessed 28.03.2025.

International Renewable Energy Agency, 2023, Innovation landscape for smart electrification: Decarbonising end-use sectors with renewable power, Abu Dhabi.

He Y., Wu H., Xu K., Zhang Y., Wang T., Wu X., Cheng C., Jin T., 2023,Theoretical performance comparison for a regenerator-enhanced three-stage auto-cascade refrigeration system using different zeotropic mixed refrigerants. Energy and Buildings, 283, 112815.

Jørgensen P. H., Elmegaard B., Zühlsdorf B., 2019, Industrial Heat Pumps, Second Phase IEA Heat Pump Technology (HPT) Programme Annex 48 Task 2: Danish Report.

Martínez-Rodríguez G., Díaz-de-León C., Fuentes-Silva A.L., Baltazar J.-C., García-Gutiérrez R., 2023, Detailed Thermo-Economic Assessment of a Heat Pump for Industrial Applications. Energies 16, 2784.

Martínez-Rodríguez G., Fuentes-Silva A.L., Baltzar J-C., 2024, Increase in Efficiency in Electric Power Production Using a Coupled System Heat Pump – Solar Thermal Installation for Industrial Applications. Chemical Engineering Transactions 114,1-6.

Martínez-Rodríguez G., Fuentes-Silva A.L., Lizárraga-Morazán J.R., Picón-Núñez M., 2019, Incorporating the Concept of Flexible Operation in the Design of Solar Collector Fields for Industrial Applications. Energies,12, 570.

Qiu K., Thomas M., 2024, Modeling and optimization of two-stage compression heat pump system for cold climate applications. Journal of Building Engineering, 82, 108407.

Schlosser F., Jesper M., Vogelsang J., Walmsley T.G., Arpagaus C., Hesselbach J., 2020, Large-scale heat pumps: Applications, performance, economic feasibility and industrial integration. Renewable and Sustainable Energy Reviews, 133, 110219.

TechNavio, 2025, Industrial Heat Pumps Market 2025-2029, <researchandmarkets.com/report/industrial-heat-pumps?utm_source=BW&utm_medium=PressRelease&utm_code=x9ptcp&utm_campaign=2010990+-+Industrial+Heat+Pump+Industry+Research+2024%3a+%249.5+Billion+Market+Trends%2c+Opportunities+and+Forecasts+2020-2024+%26+2025-2030+-+>, 28.03.2025.

United Nations Environment Programme (2024). Emissions Gap Report 2024: No more hot air … please! With a massive gap between rhetoric and reality, countries draft new climate commitments. United Nations Environment Programme. <www.undp.org/sites/g/files/zskgke326/files/2025-01/egr2024.pdf>, accessed 28.03.2025.